ACS APPLIED POLYMER MATERIALS

Editors' Choice

pubs.acs.org/acsapm

Article

Electrospun Nanofibrous Membranes from Discarded Polyester Textiles for Oil Sorption

Yelin Ko, Juan P. Hinestroza, and Tamer Uyar*

Cite This: ACS Appl. Polym. Mater. 2024, 6, 8798−8810

Read Online

ACCESS | Metrics & More | Article Recommendations | Supporting Information

ABSTRACT: The massive amounts of textile waste generated every year emphasize an urgent need for innovative strategies to repurpose discarded textiles into valuable items. We report on the fabrication of electrospun nanofibrous membranes (NFMs) utilizing discarded polyester textiles and assessing their oil sorption capabilities. We used Spandex/polyester t-shirt and polyester t-shirt sources for the NFMs. We also used a discarded poly(ethylene terephthalate) (PET) bottle to produce NFMs. The resulting NFMs were labeled as SP t-shirt NFM, PET t-shirt NFM, and PET bottle NFM. We investigated the thermal and chemical properties of the NFMs through TGA, DSC, FTIR, and XPS analyses. The SP t-shirt NFM exhibited the highest water contact angle (WCA) of 134 ± 1°, while the WCA of the PET t-shirt NFM and PET bottle NFM were 123 ± 1 and 122 ± 1°, respectively. The SP t-shirt NFM also exhibited the highest oil sorption capacity. The sorption capacities of the SP t-shirt NFM for vegetable oil, pump oil, silicone oil, and hexane were determined to be 21.4 ± 3.3, 24.1 ± 1.0, 23.7 ± 1.3, and 15.0 ± 0.5 g g^{-1}, respectively. This superior oil sorption capability of the SP t-shirt NFM is attributed to the presence of Spandex traces in the nanofibers, providing a more hydrophobic content than PET, thereby enhancing oil sorption activities. The SP t-shirt NFM exhibited satisfactory reusability as oil sorbents over five cycles and demonstrated effective adsorption of pump oil from water. This study provides valuable insights into upcycling approaches for repurposing discarded textiles into functional materials, with potential applications in addressing oil pollution problems.

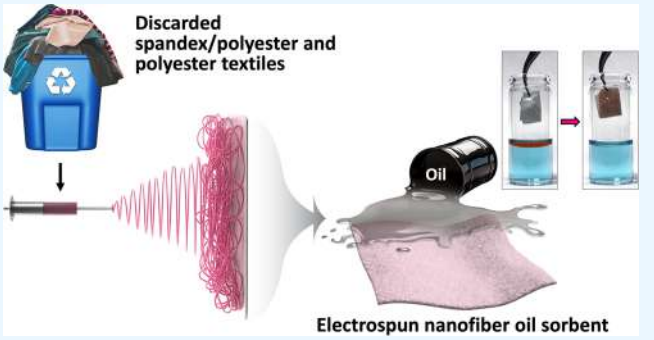

KEYWORDS: *electrospinning, nanofibrous membranes, polyester fabrics, Spandex, recycling textiles, oil sorption*

INTRODUCTION

The global annual average textile consumption per capita has doubled, increasing from 7 to 13 kg over the last 2 decades.[1] The rise in fast fashion trends has significantly shortened the lifespan of clothing items, leading to a notable increase in textile waste generation.[2] In 2015, global textile waste reached 92 million tons, which is expected to increase to 148 million tons per year by 2030.[3,4] The fact that 66% of textile waste ends up in landfills[5] has detrimental effects on the environment, particularly considering the decade-long decomposition period of man-made fibers. Addressing this environmental challenge requires innovative approaches to effectively transform discarded textiles into high-value products.

One of the leading contributors to textile waste is poly(ethylene terephthalate) (PET) fibers, commonly referred to as polyester fibers, which currently dominate the textile market. Considerable attention has been given to research aimed at developing recycling approaches for discarded PET materials across various applications.[6,7] Electrospinning leverages recycled PET (rPET) items as polymer sources to produce nanofibrous membranes (NFMs). For instance, Šišková et al. developed a nanofibrous membrane (NFM) filter as a viable alternative for face masks, utilizing PET bottles.[8] Zander et al. demonstrated applications of rPET NFMs in water filtration.[9] Additionally, Roy et al. proposed the creation of PET electrospun aerogels from PET bottles for the adsorption of heavy metal ions from contaminated water.[10] Venturelli and colleagues reported the effectiveness of their rPET NFM as a reservoir for peppermint oils.[11] Chen et al. demonstrated the efficacy of superhydrophobic and superoleophilic rPET NFMs for separating water-in-oil emulsions.[12] Furthermore, many studies utilized rPET membranes as substrates, modifying them for various other purposes.[13−16] However, these previous efforts have predominantly focused on using PET bottles to produce electrospun NFMs, overlooking the potential of discarded polyester textiles as alternative polymer sources.

Received: March 25, 2024
Revised: June 22, 2024
Accepted: June 24, 2024
Published: July 18, 2024

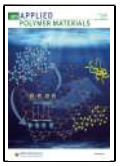

Scheme 1. Production of Electrospun NFMs Using Discarded Spandex/Polyester and Polyester Textiles, and PET Bottles for Oil Sorption Applications

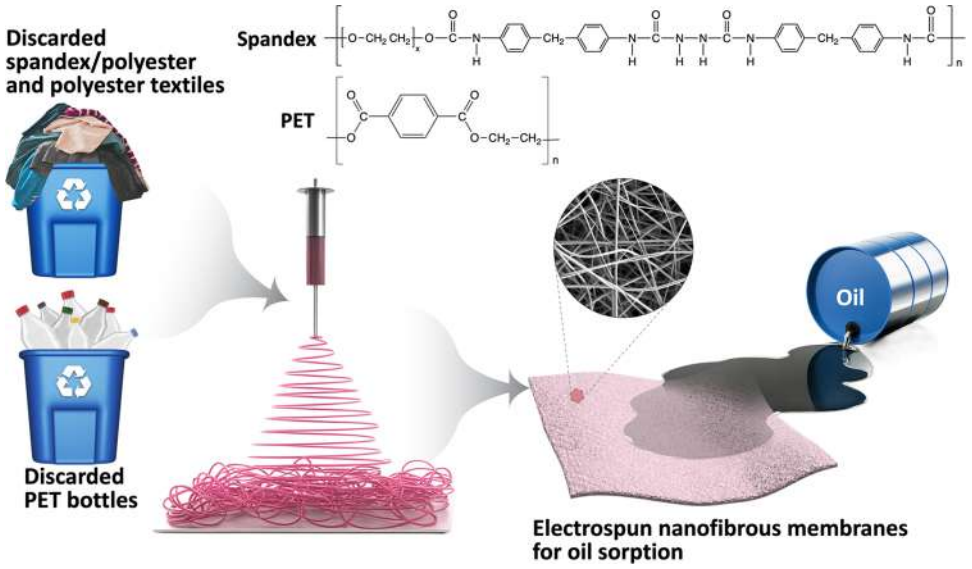

Despite numerous previous studies demonstrating various applications of electrospun rPET NFMs, the area of oil sorption has received limited attention. Recently, Topuz et al. introduced an approach to produce electrospun NFMs from PET bottles specifically for oil sorption.[17] The resulting membranes demonstrated comparable sorption performance to that of polypropylene-based commercial membranes. Their rPET NFMs achieved sorption capacities of 22.9 ± 2.0, 19.6 ± 1.8, 11.1 ± 1.0, and 19.3 ± 1.6 g g^{-1} for crude oil, diesel, gasoline, and pump oil, respectively.

In a previous study, we examined the structural differences between NFMs made from polyester textiles and PET bottles.[18] As a follow-up, we hereby present the effectiveness of electrospun NFMs produced from discarded polyester textiles for oil sorption, as shown in Scheme 1. The NFMs were produced from three different discarded polymer sources: (1) a Spandex/polyester t-shirt (SP t-shirt), (2) a polyester t-shirt (PET t-shirt), and (3) a PET bottle. Spandex fibers, illustrated in Scheme 1, are long-chain synthetic polymers primarily composed of segmented polyurethanes. The long-chain polyglycols in the soft segment impart flexibility to the fibers, while the short di-isocyanates contribute to their durability and recovery.[19] As a result, Spandex is commonly blended with polyester fibers for use in athletic clothing. Leveraging the more hydrophobic nature of Spandex over polyester, we incorporated a Spandex/polyester blend as a polymer source to enhance the oil sorption performance of the NFM sorbents. The NFMs produced from discarded textiles and PET bottles were investigated and compared for their oil sorption capacities using vegetable oil, pump oil, silicone oil, and hexane.

EXPERIMENTAL SECTION

Materials. Figure S1 shows digital photographs of discarded PET sources. A discarded 100% polyester t-shirt and a Spandex/polyester t-shirt (16% Spandex/84% polyester) were obtained from local users (Figure S1a,b). The t-shirts were washed using a commercial washer and air-dried at room temperature before use. A Coca-Cola PET bottle was cleaned after removing its label and air-dried before use (Figure S1c). Trifluoroacetic acid (TFA, Sigma-Aldrich, 99%) and dichloromethane (DCM, Sigma-Aldrich, 99.8%) were used as received without further purification. Vegetable oil was purchased from a local supermarket, pump oil from VWR, vacuum pump oil 19, silicone oil from Thomas Scientific, dimethyl silicone fluid, and hexane from Sigma-Aldrich, 99.5%.

Production of Electrospun NFMs from Discarded T-Shirts and PET Bottles. The SP t-shirt, PET t-shirt, and PET bottle were cut into small pieces. A solvent system consisting of a 70/30 mixture (by volume) of TFA and DCM was used to dissolve the discarded polymers to a concentration of 30 wt % (w/v, with respect to solvent). In our previous paper, we used a 50/50 solvent mixture of TFA and DCM.[18] In this study, we increased the TFA ratio to better dissolve Spandex fibers and produce thinner as well as more uniform fibers. Each solution exclusively contained either the SP t-shirt, PET t-shirt, or PET bottle pieces, with no intermixing between them.

The polymer solutions were stirred for 7 h at room temperature and separately loaded into 1 mL plastic syringes attached with 27 G metallic needles. An electrospinning equipment (Spingenix, model: SG100, Palo Alto) was used to produce the NFMs. Each syringe was positioned horizontally on a syringe pump, which dispensed the spinning solutions at a flow rate of 0.5 mL/h. Fibers were collected on a stationary and grounded metal collector covered with aluminum foil, located 20 cm away from the needle's tip. A voltage of 16 kV was applied to the needle. The temperature and relative humidity during the electrospinning experiments were ∼20 °C and ∼22%RH. All electrospun NFM samples were placed in a suction hood overnight, located in our laboratory, to allow for the complete evaporation of any residual solvents.

Characterization. Scanning electron microscopy (SEM) images of the NFMs were taken using a Zeiss Gemini 500 scanning electron microscope at a voltage of 2.0 kV. The NFM samples were secured on carbon tape and sputtered with a thin layer of gold−palladium prior to the measurements. Average fiber diameter (D) was determined using the ImageJ software with 100 data points, and the values are reported as a mean ± standard deviation (SD).

Thermogravimetric analysis (TGA) of the NFMs was performed using a TGA analyzer (Q500, TA Instruments). Samples were heated from 25 to 700 °C in a nitrogen atmosphere at a heating rate of 10 °C·min^{-1}. Differential scanning calorimetry (DSC) of the NFMs was recorded using a TA Instruments Q2000 system. The samples were heated from 25 to 300 °C at a heating rate of 5 °C·min^{-1}. The degree of crystallinity (% crystallinity) of the NFMs was calculated using eq 1:

https://doi.org/10.1021/acsapm.4c00916
ACS Appl. Polym. Mater. 2024, 6, 8798−8810

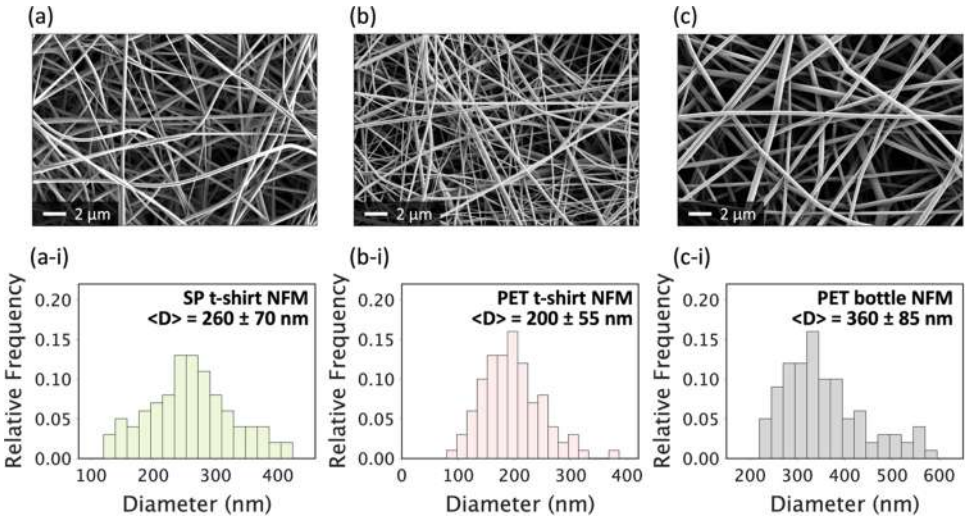

Figure 1. SEM images of (a) SP t-shirt NFM, (b) PET t-shirt NFM, and (c) PET bottle NFM. Fiber diameter distributions are presented in (a-i, b-i, and c-i) for each sample.

$$\% \text{ crystallinity} = \frac{\Delta H_m - \Delta H_{cc}}{\Delta H_c} \times 100\% \quad (1)$$

where ΔH_m is the melting enthalpy, ΔH_{cc} represents the cold crystallization enthalpy, and ΔH_c denotes the enthalpy of 100% crystalline polyester (140.1 J/g[20]). The ΔH_m and ΔH_{cc} values were obtained from the DSC measurements. The % crystallinity of the SP t-shirt NFM was calculated by dividing the value obtained from eq 1 by 0.84. This adjustment was made to consider that the SP t-shirt material comprised 84% polyester, assuming that Spandex would not contribute to crystallinity.

Fourier transform infrared (FTIR) spectra of the NFMs were acquired using a PerkinElmer FTIR spectrophotometer. Each spectrum was recorded in the range of 4000−600 cm^{-1}, with 64 scans and a resolution of 2 cm^{-1}. X-ray photoelectron spectroscopy (XPS) spectra were acquired with a ThermoFisher Scientific Nexsa G2 surface analysis system, employing a focused Al K monochromatic X-ray source (1486.6 eV). The binding energies underwent charge corrections to C 1s C−C peaks set at 284.8 eV. The XPS data were analyzed using CasaXPS.

Static water contact angle (WCA) was measured with a Rame-Hart 500 Goniometer. A 10 μL droplet of DI water was dispensed from a syringe onto each sample, with a full stroke time of 10 s. The WCA values were obtained from three measurements for each sample, and the results are presented as the mean ± SD.

Oil Sorption Test. For the oil sorption tests, we chose vegetable oil (viscosity: 87.7 cSt @ 20 °C), pump oil (viscosity: 162.8 cSt @ 20 °C), silicone oil (viscosity: 50.0 centistokes (cSt) @ 20 °C), and hexane (viscosity: 0.3 cSt) to assess the versatility of the NFMs as oil sorbents. These oils represent various types commonly encountered in practical scenarios, ranging from everyday household accidents to industrial accidents. Vegetable oil was chosen due to its widespread use in domestic and commercial settings. Pump oil was included to represent industrial oils and lubricants, while silicone oil was selected for its various applications in lubrication, personal care, and medical devices. Lastly, we included hexane to represent industrial solvents commonly found in manufacturing processes. Previous studies also have utilized these oils to evaluate the oil sorption performance of sorbents.[21−25]

The oil sorption capacity (Q_{sorp}) was determined using eq 2:

$$Q_{sorp} = \frac{m_1 - m_0}{m_0} \quad (2)$$

where m_0 represents the initial mass of the sample, while m_1 is the final mass of the sample after the oil sorption.

To determine the saturation time for oil sorption, we conducted preliminary sorption experiments on the SP t-shirt NFMs using pump oil, with contact times ranging from 0.5 to 120 min. Pump oil was chosen due to its highest viscosity, which is known to result in the slowest saturation compared to the other oils.[26] As shown in Figure S2, the SP t-shirt NFM demonstrated a sorption capacity of 19.2 g g^{-1} in less than 1 min and reached saturation after 30 min. Therefore, we selected a testing duration of 30 min or 1 h for the oil sorption experiments.

We assessed the oil sorption performance of the samples using the method originally outlined by Topuz et al.[17] Specifically, 5 mg of each sample was completely immersed in each oil. After specific times, the samples were taken out from the oil and held using tweezers in the air to allow excess oil to drain and then weighed. Samples tested with vegetable oil, pump oil, and silicone oil were left in the air for 1 min, while those tested with hexane were left for 5 s. Three replicates for each sample were tested, and the results are reported as the mean ± SD.

Sorption Kinetic Behavior. The sorption mechanism of the SP t-shirt NFM for pump oil was investigated using commonly employed models in oil sorption studies, including the pseudo-first order, pseudo-second order, Elovich, and intraparticle diffusion models.[27] Equations for each model are provided in Table S1.

RESULTS AND DISCUSSION

Morphology of the SP T-Shirt NFM, PET T-Shirt NFM, and PET Bottle NFM. Figure 1 shows the SEM images of the free-standing electrospun nanofibers produced from SP t-shirt, PET t-shirt, and PET bottle. All nanofibers exhibited bead-free morphologies.

The SP t-shirt NFM exhibited an average fiber diameter of 260 ± 70 nm (Figure 1a-i), while the PET t-shirt NFM showed a diameter of 200 ± 55 nm (Figure 1b-i). The PET bottle NFM exhibited the largest diameter of 360 ± 85 nm (Figure 1c-i). The smaller fiber diameters of the t-shirt NFMs can be attributed to the lower molecular weight of PET in t-shirts. Typically, fiber-grade PET possesses a molecular weight ranging from 15,000 to 20,000 g mol^{-1}, while bottle-grade PET falls within the range of 24,000−36,000 g mol^{-1}.[28] Lower-molecular-weight chains are often associated with fewer chain entanglements. According to Wang et al.,[29] the determined entanglement concentration (ϕ_e), which represents the critical concentration for chain entanglement, was higher for lower-molecular-weight PET. Given that we used the identical

https://doi.org/10.1021/acsapm.4c00916
ACS Appl. Polym. Mater. 2024, 6, 8798−8810

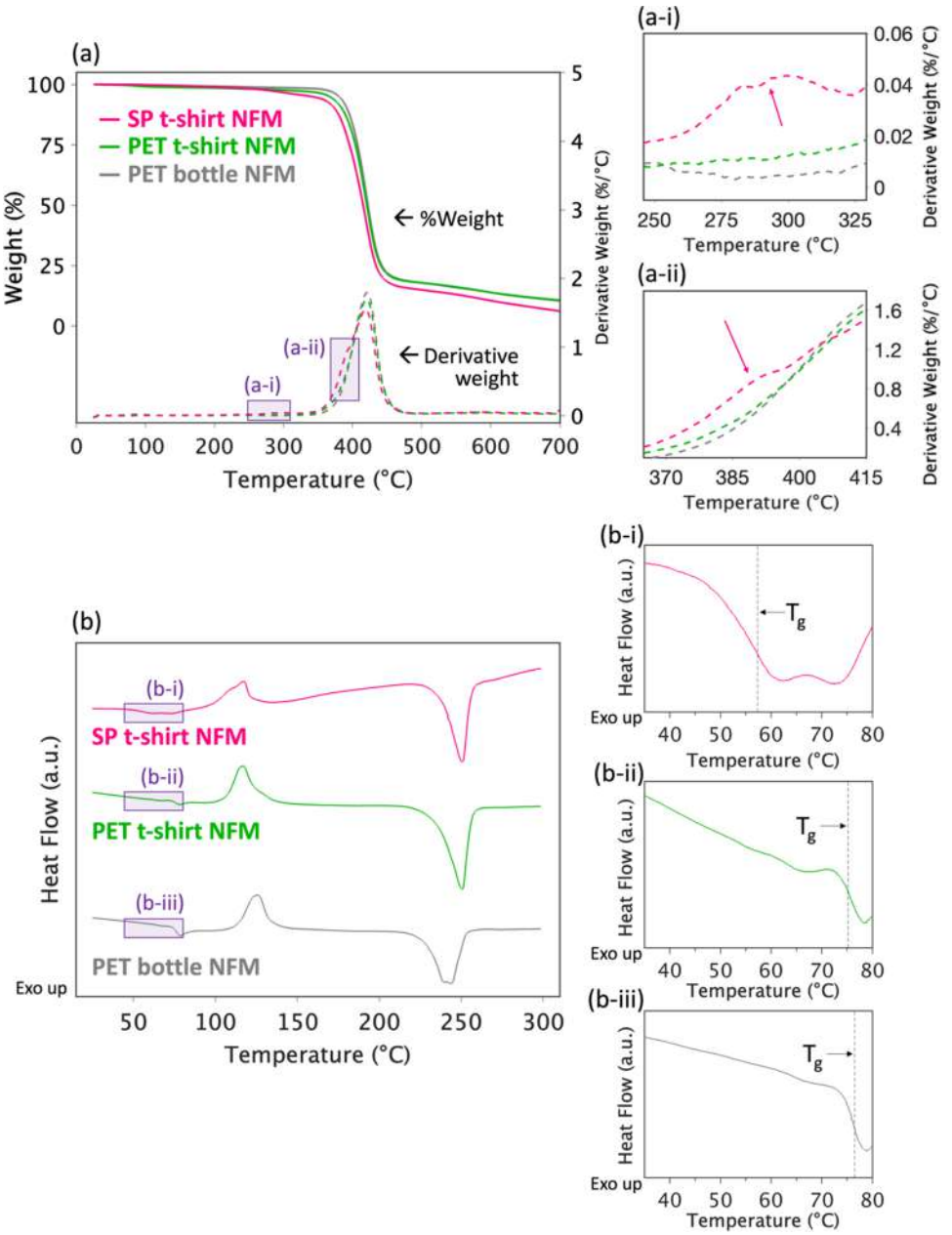

Figure 2. (a) TGA results of the SP t-shirt NFM, PET t-shirt NFM, and PET bottle NFM. Subfigures (a-i) and (a-ii) show the DTG curves of the NFMs at specified temperature ranges. (b) DSC thermograms of the SP t-shirt NFM, PET t-shirt NFM, and PET bottle NFM. Subfigures (b-i), (b-ii), and (b-iii) show the DSC curves of the NFMs at specified temperature ranges.

concentration for all solutions, it is likely that there were fewer entangled chains and lower viscosity in the t-shirt solutions. As discussed in previous papers, fewer chain entanglement and lower viscosity can lead to increased chain extensibility, thereby contributing to producing small fiber diameters.[30−33]

In addition, the smaller fiber diameters observed in the t-shirt NFMs compared to the bottle NFM can be attributed to the higher conductivity of their electrospinning solutions: 16.15 ± 0.02 μS/cm for the SP t-shirt, 19.67 ± 0.04 μS/cm for the PET t-shirt, and 0.72 ± 0.01 μS/cm for the PET bottle. The increased solution conductivity, attributable to the presence of textile dyes and additives in the t-shirts, is known to enhance jet stretching during electrospinning, thereby leading to the production of thinner fibers.[34]

As shown in Video S1, the SP t-shirt NFM demonstrated stretchability, owing to the presence of Spandex in contrast to the PET t-shirt NFM and PET bottle NFM, which were made only from PET. The observed stretchability of the SP t-shirt NFM (Video S1) aligns with the tensile test results shown in Figure S3. For comparisons, we included the tensile test data of the PET t-shirt NFM from our previous paper.[18] The SP T-shirt NFMs used for these tests were produced using the same parameters as in our earlier work.[18] As presented in Figure S3a, the SP t-shirt NFM showed a lower Young's modulus. Additionally, in the stress−strain curve shown in Figure S3b, the SP t-shirt NFM demonstrated a greater elongation at break compared to the PET t-shirt NFM.

Thermal Properties of the SP T-Shirt NFM, PET T-Shirt NFM, and PET Bottle NFM. Figure 2a shows TGA and

https://doi.org/10.1021/acsapm.4c00916
ACS Appl. Polym. Mater. 2024, 6, 8798−8810

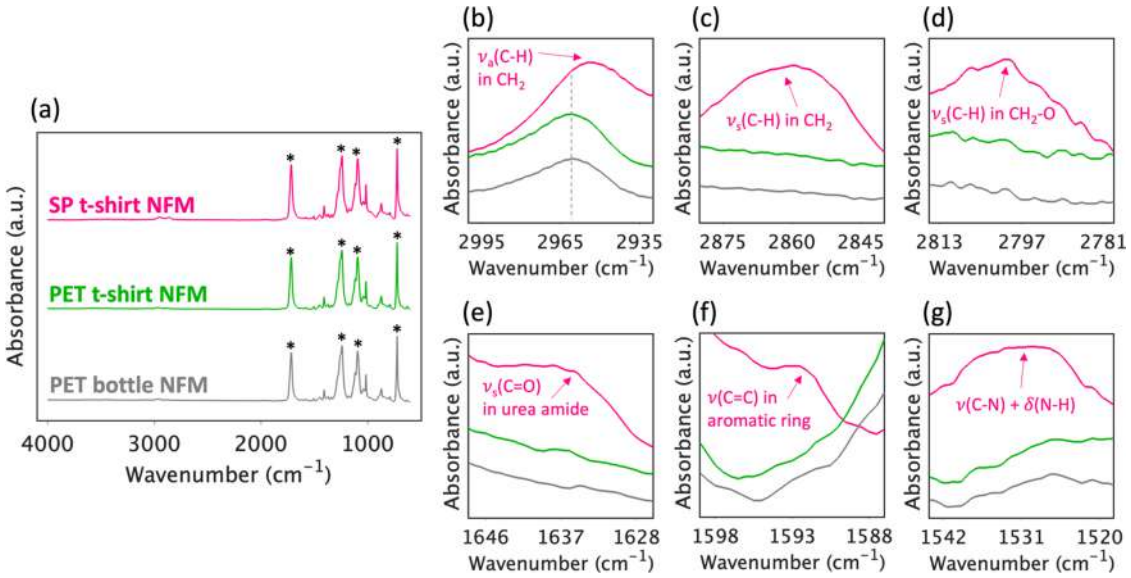

Figure 3. FTIR spectra of the SP t-shirt NFM, PET t-shirt NFM, and PET bottle NFM: (a) full scan in the range of 4000−600 cm^{-1}. Asterisks represent the characteristic peaks of PET. (b−g) Enlarged views highlight the FTIR peaks associated with Spandex, evident in the SP t-shirt NFM but absent in the PET t-shirt NFM and PET bottle NFM.

differential thermogravimetric (DTG) curves of the SP t-shirt NFM, PET t-shirt NFM, and PET bottle NFM. All NFM samples showed similar maximum decomposition temperatures (T_{max}) around 420 °C, which is in quantitative agreement with previously reported values for the T_{max} of PET.[35] The amount of residue after thermal decomposition differed, with the SP t-shirt NFM having a residue of 7.6%, while the PET t-shirt NFM and PET bottle NFM displayed values of 10.5 and 10.4%. This observation agrees with previous studies reporting a decrease in char residue with an increase in the polyurethane (PU) content of the PET/PU blend foam.[36]

Examining the DTG curves in Figure 2a-i,a-ii reveals distinctive peaks in the SP t-shirt NFM that were absent in the NFM samples made from only PET. These additional peaks can be attributed to the degradation of Spandex, which is characterized by a two-step decomposition process.[37] In particular, the peak at 295 °C in Figure 2a-i is associated with the degradation of the hard segments of Spandex consisting of urethane and urea linkages. The broad peak around 390 °C in Figure 2a-ii corresponds to the decomposition of the aliphatic ether or soft segments of Spandex. These peak values align with reported ranges for the degradation of Spandex,[37−39] indicating the presence of Spandex in the SP t-shirt NFM.

Unfortunately, due to overlaps with the degradation from PET, precise quantification of Spandex content in the SP t-shirt NFM was not achievable using TGA. Consequently, we opted to estimate the weight percentage of Spandex by examining weight loss after selectively dissolving it from the SP t-shirt NFM by DMF. The detailed procedure is provided in Figure S4. As illustrated in Figure S4b, after the selective dissolution of Spandex from the SP t-shirt NFM in DMF, the remaining SP T-shirt NFM no longer showed signs of Spandex degradation in TGA but only exhibited degradation of polyester, confirming the selective dissolution of Spandex by DMF. The weight loss after the DMF treatment of the SP T-shirt NFM was measured at 15.1 ± 2.3%, closely aligning with the labeled 16% Spandex weight in the original SP T-shirt material.

Figure 2b shows the DSC curves for the SP t-shirt NFM, PET t-shirt NFM, and PET bottle NFM. As presented in Figure 2b-i, the SP t-shirt NFM exhibited a lower glass transition temperature (T_g) of ∼60 °C compared to those for the PET t-shirt NFM at ∼75 °C (Figure 2b-ii) and the PET bottle NFM at ∼77 °C (Figure 2b-iii). This lower T_g of the SP t-shirt NFM is attributed to the presence of Spandex contents. To confirm this, we conducted a DSC analysis on commercial Spandex fibers (Glospan), as shown in Figure S5, which aligns with previous reports for Lycra.[40] A broad transition was observed between 20 and 70 °C (Figure S5), although a distinct T_g was not evident, associated with the transition of hard segments.[41] While the T_g of the soft segments of Spandex is typically observed around −60 to −70 °C,[42] that of the hard segments is not always detected;[41] however, some studies have reported T_g for these segments in the range of 40−60 °C.[37,43,44] Based on these findings, we speculate that the presence of Spandex chains in the SP t-shirt NFM enhances the overall flexibility of the polyester/Spandex matrix, leading to the observed lower T_g for the SP t-shirt NFM.

The melting temperature (T_m) values for the SP t-shirt NFM, PET t-shirt NFM, and PET bottle NFM were found to be 250.8, 250.7, and 244.1 °C, respectively, which are in agreement with reports in the scientific literature for PET's T_m.[18,45] Cold crystallization temperatures (T_{cc}) for the SP t-shirt NFM, PET t-shirt NFM, and PET bottle NFM were determined as 117.6, 117.0, and 126.0 °C, respectively. The lower T_{cc} of the t-shirt NFMs may be attributed to lower molecular weights of PET in t-shirts compared with those in bottles.[28] Some previous studies have shown that chains with fewer entanglements and greater mobility, associated with lower-molecular-weight chains, can more easily rearrange into a crystalline structure, thereby contributing to a lower T_{cc}.[46,47]

The SP t-shirt NFM and PET t-shirt NFM exhibited higher % crystallinity values of 26.3 and 19.9%, respectively, in comparison to the PET bottle NFM's value of 10.8%. The difference in crystallinity might be attributed to the lower

https://doi.org/10.1021/acsapm.4c00916
ACS Appl. Polym. Mater. 2024, 6, 8798−8810

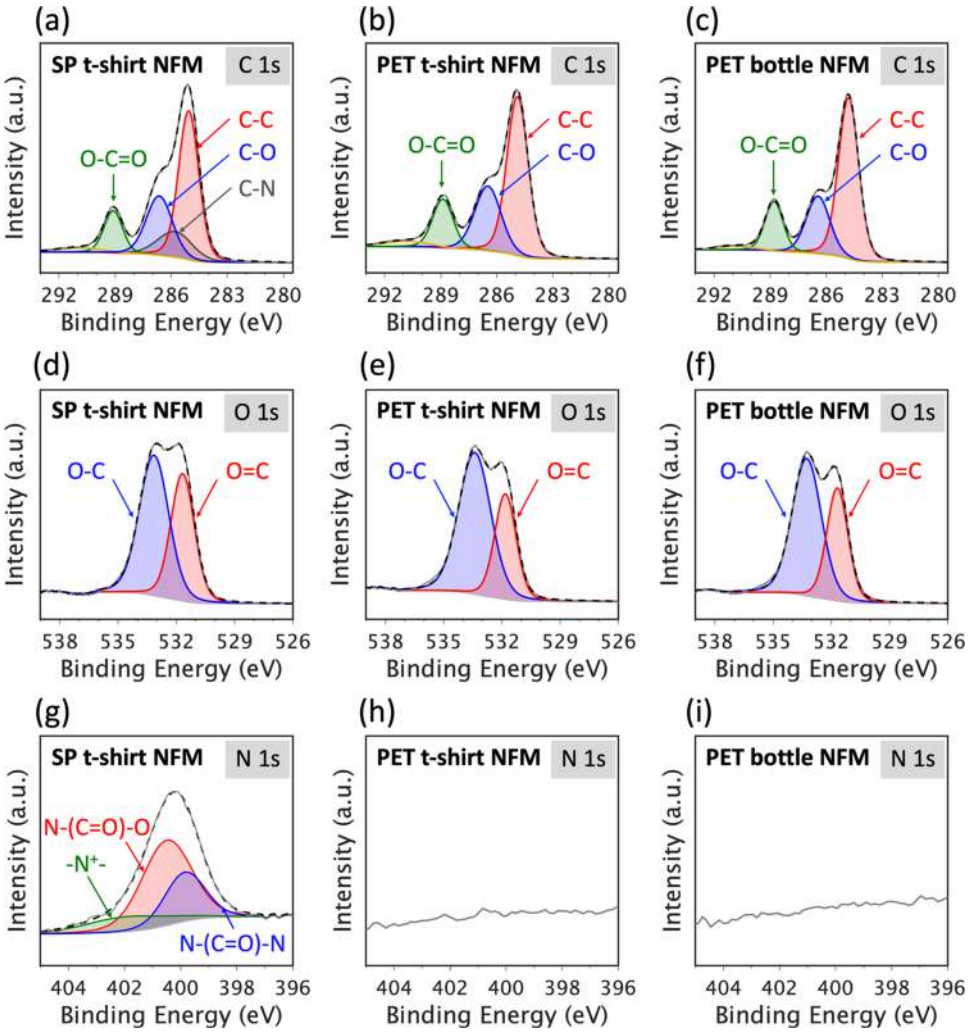

Figure 4. High-resolution XPS spectra of the SP t-shirt NFM, PET t-shirt NFM, and PET bottle NFM: (a–c) C 1s spectra, (d–f) O 1s spectra, and (g–i) N 1s spectra.

molecular weight of PET in t-shirts, as documented in previous studies,[28] which indicate that PET crystallinity tends to increase with lower molecular weight.[48] The lower molecular weight of PET likely contributed to the smaller fiber diameters for the t-shirt NFMs, as discussed in Figure 1. We speculate that the thinner fibers in the t-shirt NFMs facilitated crystallization during electrospinning. In addition, the difference in crystallinity might also be due to the presence of dye, additives, and TiO_2, which may be present in commercial textiles.

The SP t-shirt NFM displayed a higher % crystallinity compared to the PET t-shirt NFM. Samios et al. also reported that an 85%/15% PET/polyurethane polymer blend exhibited greater % crystallinity than pure PET polymer.[49] The presence of soft Spandex chains may aid in the diffusion of PET chains, thereby promoting PET crystallization during stretching via electrospinning.

Chemical and Structural Properties of the SP T-Shirt NFM, PET T-Shirt NFM, and PET Bottle NFM. Figure 3 shows the FTIR spectra of the SP t-shirt NFM, PET t-shirt NFM, and PET bottle NFM. All samples exhibited spectra consistent with those of earlier studies on PET samples[10,18] (Figure 3a). The characteristic peaks of PET are represented by asterisks in Figure 3a. The peaks identified at 1714, 1240, 1092, and 722 cm^{-1} correspond to the ester C═O group of terephthalic acid, the asymmetric stretching of the C−C−O and O−C−C groups, and the C−H wagging vibrations of the benzene ring.[45]

Figure 3b–g verifies the presence of functional groups associated with Spandex in the SP t-shirt NFM. The band assignments align with the findings of Boschmeier et al.[37] and Marchant et al.[50] In Figure 3b, the peak at 2962 cm^{-1}, observed in the PET t-shirt NFM and PET bottle NFM, shifted to a lower wavenumber in the SP t-shirt NFM. This shift can be credited to the asymmetric vibration of the C−H groups in Spandex CH_2, which is commonly found at 2938 cm^{-1}. Figure 3c,d shows peaks at 2858 and 2799 cm^{-1}, attributed to the symmetric vibration of the C−H groups in CH_2 and in CH_2−O in Spandex, respectively. New peaks emerged in the SP t-shirt NFM at 1637 and 1592 cm^{-1} (Figure 3e,f), corresponding to the symmetric vibration of the C═O groups in urea amide and the stretching vibration of the C═C moieties in the aromatic rings of Spandex. The broad band centered at 1531 cm^{-1} in Figure 3g is assigned to the C−N stretching vibration and N−H bending vibration. The peaks related to Spandex's functional groups were absent in the other NFM samples.

https://doi.org/10.1021/acsapm.4c00916
ACS Appl. Polym. Mater. 2024, 6, 8798−8810

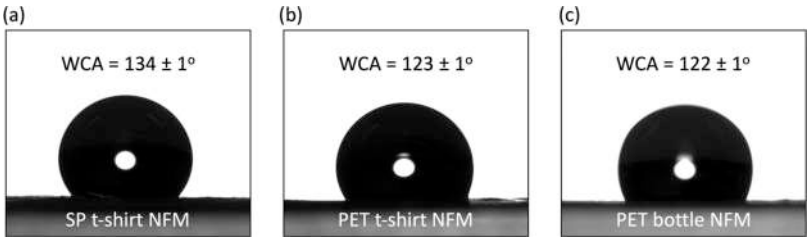

Figure 5. WCA results of the (a) SP t-shirt NFM, (b) PET t-shirt NFM, and (c) PET bottle NFM.

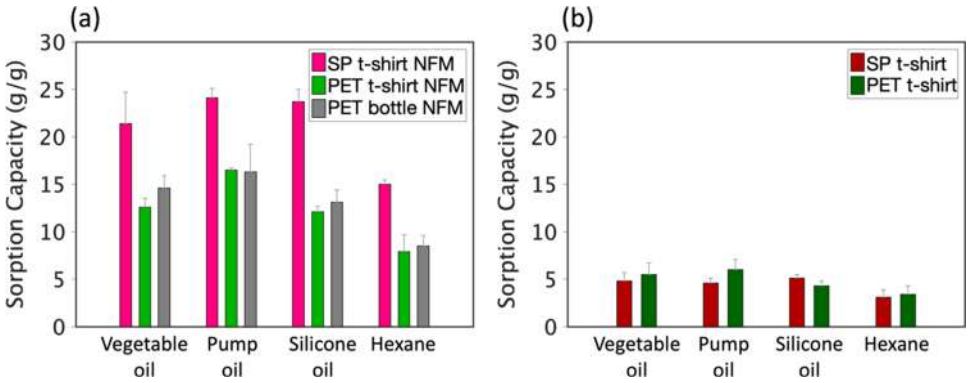

Figure 6. Sorption performance of the (a) NFMs produced from the SP t-shirt, PET t-shirt, and PET bottle, and (b) the original t-shirt fabric swatches.

XPS analysis was carried out to verify the elemental composition of PET in the NFMs and to confirm the presence of Spandex in the SP t-shirt NFM. Figure S6 shows the survey spectra of all NFM samples. Figure 4 displays the high-resolution XPS spectra and their deconvolutions. The C 1s and O 1s peaks of all NFMs were in agreement with the chemical composition peaks for PET.[17] In the C 1s spectra, subpeaks representing C−C bonds were detected at 284.8 eV, while those corresponding to O−C═O bonds were observed at 288.8 eV (Figure 4a−c). Additionally, C−O bonds were identified at 286.3 eV in the SP t-shirt NFM and at 286.4 eV in the PET t-shirt NFM as well as PET bottle NFM (Figure 4a−c). A small broad peak around 290.0 eV observed in the C 1s spectra of all NFM samples corresponds to the components of the $\pi-\pi^*$ shakeup transition associated with the aromatic ring.[51] Regarding the O 1s spectra, deconvoluted peaks were observed for O═C bonds (SP t-shirt NFM: 531.7 eV, PET t-shirt NFM: 531.8 eV, PET bottle NFM: 531.7 eV) and O−C bonds (SP t-shirt NFM: 533.1 eV, PET t-shirt NFM: 533.4 eV, PET bottle NFM: 533.3 eV) (Figure 4d−f).

The Spandex composition in the SP t-shirt NFM was confirmed using its C 1s (Figure 4a) and N 1s spectra (Figure 4g). Specifically, the SP t-shirt NFM displayed an additional C 1s subpeak at 285.5 eV (Figure 4a), attributed to C−N bonds in urethane and urea bonds.[52] In addition, the N 1s spectra of the SP t-shirt NFM displayed a discernible peak (Figure 4g), whereas the PET t-shirt NFM and PET bottle NFM did not exhibit any peaks (Figure 4h,i). The N 1s peak in the SP t-shirt NFM is deconvoluted into 399.8 (N−(C═O)−N in urea linkage),[53] 400.5 (N−(C═O)−O in urethane linkage),[53] and 401.9 eV (protonated amine),[54] indicating the presence of Spandex on the surface of the nanofibers.

Surface Wettability of the SP T-Shirt NFM, PET T-Shirt NFM, and PET Bottle NFM. While PET inherently possesses moderate hydrophobic properties, it is commonly observed that water droplets spread onto the surface of polyester fabrics after short contact. All NFM samples in our study achieved WCAs above 121° (Figure 5), with sustained hydrophobic states for over 60 min. This is attributed to the surface roughness of nanofibers as well as the inherent hydrophobicity of PET.[55] Notably, the SP t-shirt NFM achieved a significantly higher WCA of 134 ± 1° compared to that of the PET t-shirt NFM (123 ± 1°) and PET bottle NFM (122 ± 1°). The greater hydrophobicity of the SP t-shirt NFM can be credited to the Spandex content, resulting from the presence of the long and nonpolar hydrocarbon chains in its soft segments.[56] Jasmee et al. demonstrated that thermoplastic polyurethane films showed WCA of 95.4 ± 1.5°, while PET films exhibited lower values of WCA at 75.3 ± 1.2°.[57]

It is worth noting that the surface of the original SP t-shirt material was primarily composed of polyester fibers. As illustrated in Figure S7, the SP t-shirt fibers exhibit a structure where polyester fibers surround the Spandex fibers. When polymers are dissolved, the resulting solution becomes a homogeneous state. Consequently, the surface of the SP t-shirt NFM would have incorporated not only polyester but also Spandex, as supported by our XPS studies in Figure 4. We assume that the presence of Spandex contributes to enhanced hydrophobicity in the SP t-shirt NFM compared to the other NFMs.

Oil Sorption Performance of NFMs and Original T-Shirts. The oil sorption performance of the NFMs and their original t-shirt materials were evaluated using vegetable oil, pump oil, silicone oil, and hexane. The sorption capacity of the original PET bottle was not examined as it is a solid film. According to Figure 6a,b, it is evident that the NFMs exhibited significantly higher sorption capacities compared to the corresponding t-shirt fabric swatches. The SP t-shirt NFM and PET t-shirt NFM showed Q_{sorp} values 3−5 and 2−3 times higher than their corresponding original fabric sources, respectively. This is attributed to the larger surface area to volume ratio of NFMs.[58] The higher specific surface area of the

https://doi.org/10.1021/acsapm.4c00916
ACS Appl. Polym. Mater. 2024, 6, 8798−8810

Table 1. Oil Sorption Performance of Nanofibrous Membranes

sorbent material	sorption time (min)	sorption capacity (g g^{-1})				ref
		vegetable oil	pump oil	silicone oil	hexane	
rPET bottle NFM	60		19.3			17
CA/activated carbon nanofibers	60		8.3			62
CA/cellulose nitrate/carbon black nanofibers	60		13.67			63
PLA/SiO_2 nanofibers	not given				19.9	25
intrinsically microporous fluorinated polyimide nanofibers	60			~35		64
nanoporous PLA	10	28.17	42.4			21
macroporous carbonized polyacrylonitrile nanofibers	10	94.0	73.8	138.4		22
nanoporous polystyrene nanofibers	600	127.52				23
nanoporous CA butyrate nanofibers	90		60			24
SP t-shirt NFM	60	21.4	24.1	23.7	15.0	this work
PET t-shirt NFM	60	12.6	16.5	12.1	7.9	this work
PET bottle NFM	60	14.6	16.3	13.1	8.5	this work

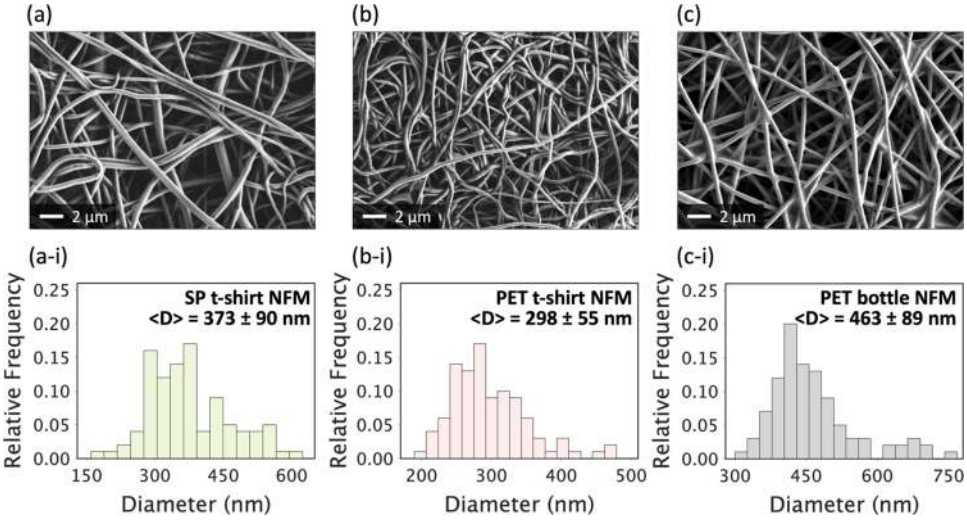

Figure 7. SEM images of the (a) SP t-shirt NFM, (b) PET t-shirt NFM, and (c) PET bottle NFM after adsorption of pump oil for 24 h. Fiber diameter distributions are presented in (a-i, b-i, and c-i) for each sample.

NFMs correlates with larger interfiber voids and increased porosity, facilitating efficient oil retention within the structure.[59,60] Additionally, smaller fiber diameters of electrospun NFMs contribute to faster oil uptake and greater oil adsorption.[61]

The SP t-shirt NFM demonstrated 1.5−2 times greater oil sorption capacities than the PET t-shirt NFM and PET bottle NFM across all tested oils, as shown in Figure 6a. We attribute the superior oil sorption performance of the SP t-shirt NFM to its enhanced hydrophobicity. Hydrophobicity is widely acknowledged as a key factor contributing to increased oil sorption performance.[61] The presence of Spandex content in the SP t-shirt NFM, as confirmed by our TGA, FTIR, and XPS analyses, likely played a role in improving the hydrophobicity of the materials, as demonstrated in our WCA results. It is worth noting that the sorption capacity of the original SP t-shirt did not outperform that of the original PET t-shirt. This is attributed to the structure of the original SP t-shirt material, as shown in Figure S7a,b, where the Spandex fibers are surrounded by polyester fibers. In contrast, the Spandex content in the SP t-shirt NFM was present on the surface as well, as confirmed by our XPS results.

Table 1 summarizes oil sorption capacity values reported in some of the previous studies, as well as those for the SP t-shirt NFM, PET t-shirt NFM, and PET bottle NFM. The oil sorption performances of the NFMs were either comparable to or outperformed those of rPET bottle NFM,[17] cellulose acetate (CA)/activated carbon nanofibers,[62] CA/cellulose nitrate/carbon black nanofibers,[63] polylactic acid/SiO_2 nanofibers,[25] and intrinsically microporous fluorinated polyimide nanofibers.[64] However, compared to nanofibers with deliberately engineered porous structures within the fibers,[21−24] the sorption performance of the SP t-shirt NFM, PET t-shirt NFM, and PET bottle NFM was lower. Future investigations may explore the potential of porosity engineering approaches for electrospun NFMs produced from textiles.

According to Sarbatly et al., thinner fibers display greater oil sorption capacity due to numerous interconnected voids.[61] However, our study did not observe this trend: the thinner PET t-shirt NFM (200 ± 55 nm) did not outperform the thicker PET bottle NFM (360 ± 85 nm). To investigate this discrepancy, we produced thicker fibers for both PET t-shirt and PET bottle NFM and evaluated their oil sorption performance using pump oil. The thicker PET t-shirt NFM was produced with a 50% w/v concentration and a 50/50 TFA/DCM ratio, while the thicker PET bottle NFM was produced using a 40% w/v and the same solvent ratio. SEM images and fiber diameter distributions are shown in Figure S8.

Consistent with previous studies, the thicker NFMs showed lower oil sorption performance. Specifically, the thicker PET t-

https://doi.org/10.1021/acsapm.4c00916
ACS Appl. Polym. Mater. 2024, 6, 8798−8810

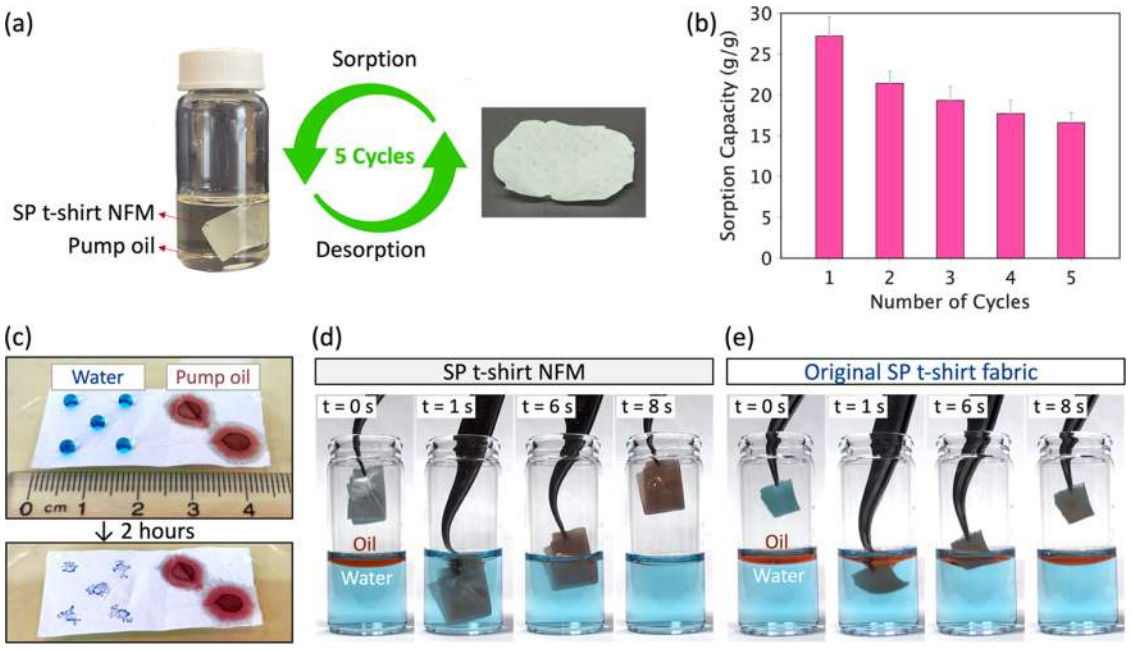

Figure 8. (a) Adsorption/desorption cyclic test of the SP t-shirt NFM. (b) Sorption capacities of the SP t-shirt NFM for pump oil during five consecutive sorption/desorption cycles. (c) Digital photograph of water (blue) and pump oil (red) droplets on the surface of the SP t-shirt NFM. (d) SP t-shirt NFM's adsorption of pump oil (red) from water (blue). (e) Original SP t-shirt swatch's adsorption of pump oil (red) from water (blue).

shirt NFM (440 ± 110 nm) had an oil sorption capacity of 12.5 ± 3.7 g g^{-1}, lower than that of the original PET t-shirt NFM (16.5 ± 0.2 g g^{-1}). The thicker PET bottle NFM (810 ± 310 nm) had an oil sorption capacity of 10.5 ± 0.4 g g^{-1}, lower than that of the original PET bottle NFM (16.3 ± 2.9 g g^{-1}). Therefore, we speculate that the influence of fiber diameter on oil sorption capacity might not be noticeable in the thinner fibers of the PET t-shirt NFM and PET bottle NFM, but it could become more pronounced as the fiber diameter increases.

As shown in Figure 6a, all NFMs exhibited the lowest adsorption performance for hexane compared to the other oils. This discrepancy can be attributed to hexane's small molecular size and lack of polar functional groups, which lead to limited intermolecular interactions and low viscosity. Hexane is recognized for its very low viscosity, 0.3 cSt, significantly lower than the measured values of the other oils (vegetable oil: 87.7 cSt; pump oil: 162.8 cSt; silicone oil: 50.0 cSt). As Sarbatly et al. noted, oils with low viscosity struggle to adhere to the fiber's surface, thereby contributing to the limited adsorption performance of the fiber sorbents.[61]

The morphologies of the SP t-shirt NFM, PET t-shirt NFM, and PET bottle NFM were examined after oil sorption, and shown in Figure 7. After immersing the NFM sorbents in pump oil for 24 h, they were retrieved and lightly pressed with paper towels. Additionally, the sorbents were immersed in ethanol for 45 min to eliminate any residual oil. The NFMs were gently pressed with paper towels again and air-dried at room temperature overnight prior to characterization. As illustrated in Figure 7, the fibers retained their overall structures after oil sorption but exhibited swelling. Consistent with findings by Topuz et al.,[17] the fiber diameters of the NFMs increased after 24 h of oil sorption. The SP t-shirt NFM showed an increase from 260 ± 70 nm (Figure 1a) to 373 ± 90 nm (Figure 7a), and the PET t-shirt NFM exhibited an increase from 200 ± 55 nm (Figure 1b) to 298 ± 55 nm (Figure 7b). Finally, the PET bottle NFM displayed an increase from 360 ± 85 nm (Figure 1c) to 463 ± 89 nm (Figure 7c).

Sorption Kinetics and Reusability of SP T-Shirt NFM, and Its Effective Oil Sorption from Water. Figure S9a–d shows the kinetic plots for the SP t-shirt NFM in pump oil, using the pseudo-first-order, pseudo-second-order, Elovich, and intraparticle diffusion models. The pseudo-second-order model provided the best fit, with an R_2 value of 0.9998 (Figure S9b), indicating a strong agreement between the observed oil sorption process and the model. The maximum oil sorption capacity was determined to be 25.5 g g^{-1}, and the pseudo-second-order rate constant was 0.06192.

To assess the reusability of the SP t-shirt NFMs, their adsorption and desorption capabilities were tested using pump oil, as presented in Figure 8a. A five-cycle reusability test was chosen, as it is a widely accepted practice in previous studies.[17,65,66] Initially, 5 mg of the SP t-shirt NFM was immersed in pump oil for 30 min and then retrieved. The NFMs were gently compressed with paper towels, rinsed with ethanol, and air-dried overnight at room temperature. These dried sorbents were reused in the next cycle of oil sorption testing. As shown in Figure 8b, the SP t-shirt NFMs demonstrated satisfactory oil adsorption performance over successive five cycles, despite experiencing a slight decrease in sorption capacity values. This decrease in oil sorption performance after repeated uses has been frequently documented in previous studies[17,64,66] that utilized mechanical recovery methods for sorbent desorption.

We did not conduct further testing after the five cycles, as this number of cycles was sufficient to demonstrate that the SP t-shirt NFM had a significantly higher accumulated oil sorption capacity compared to commercial PP sorbents, which typically exhibit a sorption capacity of 10 g g^{-1}.[66]

https://doi.org/10.1021/acsapm.4c00916
ACS Appl. Polym. Mater. 2024, 6, 8798−8810

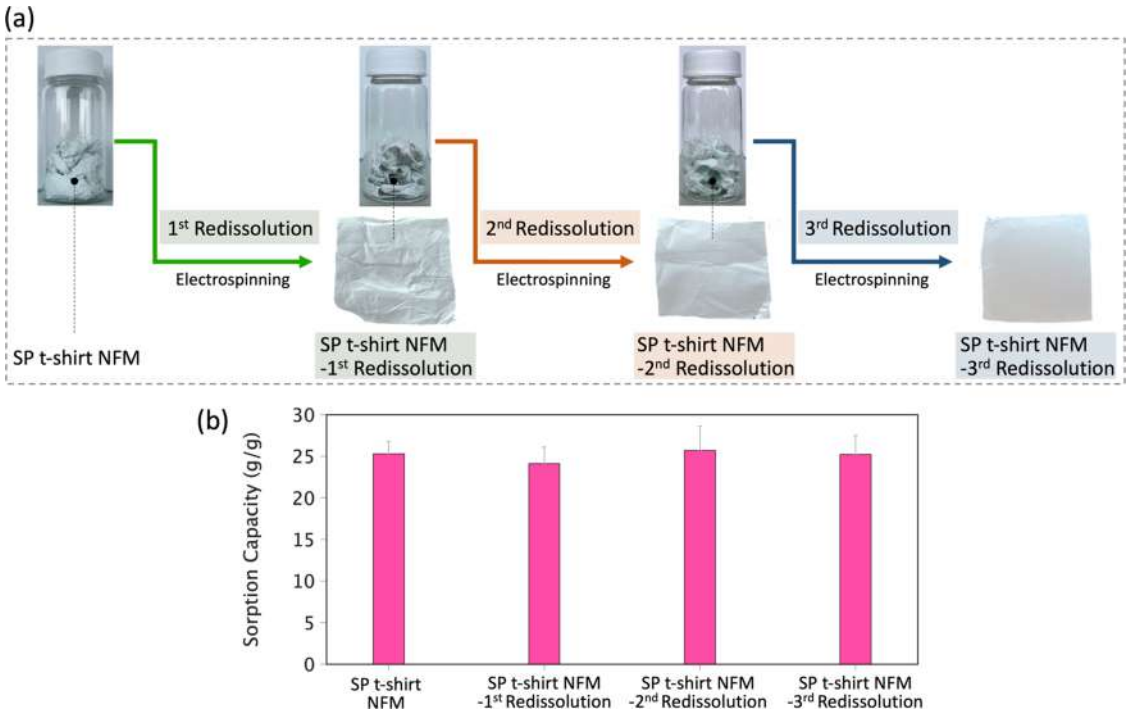

Figure 9. (a) Redissolution process for the SP t-shirt NFM to produce recycled NFMs. (b) Sorption capacities of the SP t-shirt NFM-1st, -2nd, and -3rd Redissolution for pump oil.

Figure 8c presents digital photographs showing water and pump oil droplets on the surface of the SP t-shirt NFM. To enhance visibility, methylene blue was used to dye the water droplets, while dispersed red 011 colored the oil droplets. The oil droplets immediately spread onto the membrane, while the water droplets maintained their spherical shapes on the NFM surface. After 2 h, the water droplets evaporated, leaving behind faint traces of blue dye without spreading, indicating the lasting hydrophobic nature of the SP t-shirt NFM.

The adsorption capability of the SP t-shirt NFM for pump oil from water was evaluated using a 15 mg membrane. To provide a comparison, an original SP t-shirt swatch, also weighing 15 mg, underwent the same test. As shown in Figure S10, the SP t-shirt NFM exhibited a significantly larger surface area compared to the original fabric material. Each sorbent was immersed in a mixture of water and pump oil to remove the oil component. Oil was colored with acid red 1, while methylene blue was used to dye water. Figure 8d demonstrates that the SP t-shirt NFM effectively removed pump oil from the water within 5 s. In contrast, as shown in Figure 8e, the original SP t-shirt swatch displayed limited adsorption capabilities compared to the SP t-shirt NFM. These results suggest the promising potential for textile-sourced NFMs in the separation of oil from aqueous systems. Videos demonstrating the performance of the SP t-shirt NFM in adsorbing pump oil from water, as well as its comparison with the original fabric swatch, are available in Videos S2 and S3.

Stability and Recyclability Test of the SP T-Shirt NFM to Mitigate Disposal Issues. Nanoplastics, including residues of nanofibers, are recognized for their potential toxicity on the digestive, reproductive, and nervous systems.[67] Therefore, evaluating the structural integrity of the SP t-shirt NFM in oil over an extended period may be crucial. An SP t-shirt NFM was weighed (Figure S11a) and immersed in pump oil under magnetic stirring at room temperature (Figure S11b). After 24 h, the membrane was removed from the oil. As shown in Figure S11c, visual inspection revealed no observable signs of residual nanofibers disintegrating in the oil. Subsequently, the membrane was gently compressed and rinsed with hexane to remove any adsorbed oil from the fiber surface. The resulting membrane showed a weight change of 0.01 ± 0.02 mg compared to its initial weight, indicating no significant weight loss (Figure S11d).

Effective recycling strategies for electrospun NFMs may help minimize secondary pollution issues associated with NFM disposal. To explore this potential, we investigated recycling SP t-shirt NFM by using it as a polymer source for another NFM. In Figure 9a, we demonstrate the process: the SP t-shirt NFM was redissolved into TFA/DCM solvents, and the resulting solution was electrospun to create another SP t-shirt NFM, referred to as SP t-shirt NFM-1st Redissolution. This membrane was then dissolved and used as a polymer source for another SP t-shirt NFM, named SP t-shirt NFM-2nd Redissolution. Finally, this membrane was utilized to produce another NFM, called SP t-shirt NFM-3rd Redissolution.

Figure 9b shows the oil sorption performance of the three recycled NFMs, tested for 30 min in pump oil. All recycled NFMs exhibited a comparable oil sorption capacity to that of the original SP t-shirt NFM. This finding suggests that repurposing NFMs as raw materials to produce other NFMs could serve as a potential recycling strategy to mitigate risks related to NFM disposal.

CONCLUSIONS

We demonstrated a potential application for electrospun nanofibrous membranes produced from a discarded Spandex/polyester t-shirt, a polyester t-shirt, and a PET bottle. The presence of Spandex in the Spandex/polyester t-shirt NFM was confirmed through TGA, FTIR, and XPS analyses. The NFM sorbents produced from the Spandex/polyester t-shirt were

https://doi.org/10.1021/acsapm.4c00916
ACS Appl. Polym. Mater. 2024, 6, 8798−8810

able to adsorb vegetable oil, pump oil, silicone oil, and hexane in capacities that were 1.5−2.0 times higher than those of the NFMs produced from the polyester t-shirt and the PET bottle, which did not contain Spandex content. This superior oil sorption performance of the Spandex/polyester t-shirt NFM was attributed to improved hydrophobicity resulting from the Spandex content, as supported by higher water contact angle values. The SP t-shirt NFMs demonstrated satisfactory reusability as oil sorbents over five consecutive cycles while also proving effective in adsorbing pump oil from water. Our findings suggest an innovative strategy for repurposing discarded polyester Spandex textiles into valuable products. This is quite relevant as athletic and flexible clothing are one of the fastest-growing segments of apparel sales, and they are mostly manufactured with polyester and increasing amounts of Spandex.

■ ASSOCIATED CONTENT

Supporting Information

The Supporting Information is available free of charge at https://pubs.acs.org/doi/10.1021/acsapm.4c00916.

Digital photograph of the Spandex/polyester t-shirt, polyester t-shirt, and PET bottle (Figure S1); oil saturation test for the SP t-shirt NFM (Figure S2); tensile testing of the NFMs (Figure S3); selective dissolution of Spandex in the SP t-shirt NFM (Figure S4); DSC thermogram for commercial Spandex (Figure S5); XPS survey spectra of the NFMs (Figure S6); cross-sectional image of the original Spandex/polyester t-shirt material (Figure S7); SEM images and fiber diameter distributions of the thicker PET t-shirt NFM and PET bottle NFM (Figure S8); sorption kinetic plots of the SP t-shirt NFM for pump oil (Figure S9); digital photograph of the SP t-shirt NFM and the original Spandex/polyester t-shirt swatch weighing 15 mg each (Figure S10); stability testing of the SP t-shirt NFM (Figure S11); and equations and parameters for the sorption kinetic model (Table S1) (PDF)

Video S1: demonstration of the stretchability of the SP t-shirt NFM compared to the PET t-shirt NFM and PET bottle NFM. (MP4)

Video S2: pump oil adsorption performance of the SP t-shirt NFM. (MP4)

Video S3: pump oil adsorption performance of the original SP t-shirt fabric swatch. (MP4)

■ AUTHOR INFORMATION

Corresponding Author

Tamer Uyar − *Fiber Science Program, Department of Human Centered Design, College of Human Ecology, Cornell University, Ithaca, New York 14853, United States;* orcid.org/0000-0002-3989-4481; Email: tu46@cornell.edu

Authors

Yelin Ko − *Fiber Science Program, Department of Human Centered Design, College of Human Ecology, Cornell University, Ithaca, New York 14853, United States*

Juan P. Hinestroza − *Fiber Science Program, Department of Human Centered Design, College of Human Ecology, Cornell University, Ithaca, New York 14853, United States;* orcid.org/0000-0001-7452-2635

Complete contact information is available at: https://pubs.acs.org/10.1021/acsapm.4c00916

Author Contributions

Y.K. produced samples, performed characterizations, analyzed and visualized the data, and wrote the initial draft. J.P.H. provided guidance on data interpretation and edited the manuscript. T.U. provided initial planning of the experiments, guided data analysis, and edited the manuscript. The manuscript was written through the contributions of all authors. All authors have reviewed and approved the final version of the manuscript.

Notes

The authors declare no competing financial interest.

■ ACKNOWLEDGMENTS

This work utilized the Cornell Center for Materials Research Shared Facilities, which are supported through the NSF MRSEC program (DMR-1719875), and the Department of Human Centered Design Facilities. Y.K. acknowledges financial support for this research from the Fulbright U.S. Student Program, which is sponsored by the U.S. Department of State and the Korean-American Educational Commission. The views expressed in this work are solely those of the author and do not necessarily represent the views of the Fulbright Program, the U.S. Government, or the Korean-American Educational Commission.

■ REFERENCES

(1) Shirvanimoghaddam, K.; Motamed, B.; Ramakrishna, S.; Naebe, M. Death by Waste: Fashion and Textile Circular Economy Case. *Sci. Total Environ.* **2020**, *718*, No. 137317.

(2) Gupta, R.; Kushwaha, A.; Dave, D.; Mahanta, N. R. Waste Management in Fashion and Textile Industry: Recent Advances and Trends, Life-Cycle Assessment, and Circular Economy. In *Emerging Trends to Approaching Zero Waste*; Elsevier, 2022; pp 215−242.

(3) Kamble, Z.; Behera, B. K. Upcycling Textile Wastes: Challenges and Innovations. *Text. Prog.* **2021**, *53* (2), 65−122.

(4) Textile Exchange. Preferred Fiber & Materials Market Report 2021 https://textileexchange.org/app/uploads/2021/08/Textile-Exchange_Preferred-Fiber-and-Materials-Market-Report_2021.pdf (accessed May 21, 2024).

(5) Environmental Protection Agency (EPA). Advancing Sustainable Materials Management: 2014 Fact Sheet 2015 https://www.epa.gov/sites/default/files/2016-11/documents/2014_smmfactsheet_508.pdf (accessed May 21, 2024).

(6) Sadeghi, B.; Marfavi, Y.; AliAkbari, R.; Kowsari, E.; Borbor Ajdari, F.; Ramakrishna, S. Recent Studies on Recycled PET Fibers: Production and Applications: A Review. *Mater. Circ. Econ.* **2021**, *3*, 4.

(7) Ren, T.; Zhan, H.; Xu, H.; Chen, L.; Shen, W.; Xu, Y.; Zhao, D.; Shao, Y.; Wang, Y. Recycling and High-Value Utilization of Polyethylene Terephthalate Wastes: A Review. *Environ. Res.* **2024**, *249*, No. 118428.

(8) Šišková, A. O.; Frajová, J.; Nosko, M. Recycling of Poly (Ethylene Terephthalate) by Electrospinning to Enhanced the Filtration Efficiency. *Mater. Lett.* **2020**, *278*, No. 128426.

(9) Zander, N. E.; Gillan, M.; Sweetser, D. Recycled PET Nanofibers for Water Filtration Applications. *Materials* **2016**, *9* (4), 247.

(10) Roy, S.; Maji, P. K.; Goh, K. L. Sustainable Design of Flexible 3D Aerogel from Waste PET Bottle for Wastewater Treatment to Energy Harvesting Device. *Chem. Eng. J.* **2021**, *413*, No. 127409.

(11) Venturelli, R. B.; Immich, A. P. S.; Ma, G.; de Souza, S.; de Souza, A. A. Recycled Polyester Nanofiber as a Reservoir for Essential Oil Release. *J. Appl. Polym. Sci.* **2021**, *138* (16), No. 50258.

(12) Chen, H.; Zuo, Z.; Tian, Q.; Xue, S.; Qiu, F.; Peng, X.; Zhang, T. Waste to Treasure: A Superwetting Fiber Membrane from Waste

PET Plastic for Water-in-Oil Emulsion Separation. *J. Cleaner Prod.* **2023**, *396*, No. 136502.
(13) Jiang, Z.; Piao, S.; Park, T.; Li, S.; Kim, Y.; Lee, E.; Bae, C.; Lee, Y.; Im, H.; Oh, J.; et al. Multifunctional Ultrathin Recycled PET-Based Membrane for Electromagnetic Interference Shielding, Antibacterial and Thermal Management. *Adv. Mater. Interfaces* **2024**, *11*, No. 2301047.
(14) Fulton, A. C.; Thum, M. D.; Jimenez, J.; Camarella, G.; Cilek, J. E.; Lundin, J. G. Long-Term Insect Repellent Electrospun Microfibers from Recycled Poly (Ethylene Terephthalate). *ACS Appl. Mater. Interfaces* **2023**, *15* (38), 44722−44730.
(15) Kijeńska-Gawrońska, E.; Zdarta, J.; Thabit, H. S. A. M.; Jesionowski, T.; Swieszkowski, W. From PET Bottle Waste to Enzyme Support for Removal of Estrogens from Wastewaters. *Environ. Technol. Innovations* **2024**, *34*, No. 103555.
(16) Zhu, S.; Jia, X.; Ni, Y.; Pan, B.; Long, Y.; Miao, D.; Yan, X. A 3D Solar-Driven Evaporator Based on Electrospun Recycled PET Film for Efficient Seawater Desalination. *J. Cleaner Prod.* **2023**, *408*, No. 137113.
(17) Topuz, F.; Oldal, D. G.; Szekely, G. Valorization of Polyethylene Terephthalate (PET) Plastic Wastes as Nanofibrous Membranes for Oil Removal: Sustainable Solution for Plastic Waste and Oil Pollution. *Ind. Eng. Chem. Res.* **2022**, *61* (25), 9077−9086.
(18) Ko, Y.; Hinestroza, J. P.; Uyar, T. Structural Investigation on Electrospun Nanofibers from Postconsumer Polyester Textiles and PET Bottles. *ACS Appl. Polym. Mater.* **2023**, *5* (9), 7298−7307.
(19) Hu, J.; Lu, J.; Zhu, Y. New Developments in Elastic Fibers. *Polym. Rev.* **2008**, *48* (2), 275−301.
(20) Varma-Nair, M.; Wunderlich, B. Heat Capacity and Other Thermodynamic Properties of Linear Macromolecules X. Update of the ATHAS 1980 Data Bank. *J. Phys. Chem. Ref. Data* **1991**, *20* (2), 349−404.
(21) Liang, J. W.; Prasad, G.; Wang, S. C.; Wu, J. L.; Lu, S. G. Enhancement of the Oil Absorption Capacity of Poly (Lactic Acid) Nano Porous Fibrous Membranes Derived via a Facile Electrospinning Method. *Appl. Sci.* **2019**, *9* (5), 1014.
(22) Liu, H.; Cao, C. Y.; Wei, F. F.; Huang, P. P.; Sun, Y. B.; Jiang, L.; Song, W. G. Flexible Macroporous Carbon Nanofiber Film with High Oil Adsorption Capacity. *J. Mater. Chem. A* **2014**, *2* (10), 3557−3562.
(23) Jia, M.; Liu, H.; Yang, G.; Zhang, S.; Yang, J.; Tian, L.; Zhu, C.; Xu, J. Biomimetic Porous Nanofiber-Based Oil Pump for Spontaneous Oil Directional Transport and Collection. *ACS Appl. Mater. Interfaces* **2021**, *13* (14), 16887−16894.
(24) Tanvir, A.; Ting, V. P.; Eichhorn, S. J. Nanoporous Electrospun Cellulose Acetate Butyrate Nanofibres for Oil Sorption. *Mater. Lett.* **2020**, *261*, No. 127116.
(25) Ye, B.; Jia, C.; Li, Z.; Li, L.; Zhao, Q.; Wang, J.; Wu, H. Solution-blow Spun PLA/SiO_2 Nanofiber Membranes toward High Efficiency Oil/Water Separation. *J. Appl. Polym. Sci.* **2020**, *137* (37), No. 49103.
(26) Qiao, Y.; Zhao, L.; Li, P.; Sun, H.; Li, S. Electrospun Polystyrene/Polyacrylonitrile Fiber with High Oil Sorption Capacity. *J. Reinf. Plast. Compos.* **2014**, *33* (20), 1849−1858.
(27) Piperopoulos, E.; Calabrese, L.; Mastronardo, E.; Abdul Rahim, S. H.; Proverbio, E.; Milone, C. Assessment of Sorption Kinetics of Carbon Nanotube-based Composite Foams for Oil Recovery Application. *J. Appl. Polym. Sci.* **2019**, *136* (14), No. 47374.
(28) Rieckmann, T.; Völker, S. Poly(Ethylene Terephthalate) Polymerization − Mechanism, Catalysis, Kinetics, Mass Transfer and Reactor Design. In *Modern Polyesters: Chemistry and Technology of Polyesters and Copolyesters*; John Wiley & Sons, 2005; pp 35−36.
(29) Wang, C.; Lee, M. F.; Wu, Y. J. Solution-Electrospun Poly (Ethylene Terephthalate) Fibers: Processing and Characterization. *Macromolecules* **2012**, *45* (19), 7939−7947.
(30) Yang, Y.; Li, X.; Mi, J.; Ramakrishna, S.; Ji, D.; Yu, J.; Wang, R.; Qin, X. Coordinating Chain Crystallinity and Orientation by Tailoring Electrical Stretching for Fabrication of Super-Tough and Strong Organic Fibers. *Chem. Eng. J.* **2022**, *442*, No. 136203.
(31) Wang, C.; Fang, C. Y.; Wang, C. Y. Electrospun Poly (Butylene Terephthalate) Fibers: Entanglement Density Effect on Fiber Diameter and Fiber Nucleating Ability towards Isotactic Polypropylene. *Polymer* **2015**, *72*, 21−29.
(32) Shenoy, S. L.; Bates, W. D.; Frisch, H. L.; Wnek, G. E. Role of Chain Entanglements on Fiber Formation during Electrospinning of Polymer Solutions: Good Solvent, Non-Specific Polymer−Polymer Interaction Limit. *Polymer* **2005**, *46* (10), 3372−3384.
(33) Ojha, S. S.; Afshari, M.; Kotek, R.; Gorga, R. E. Morphology of Electrospun Nylon-6 Nanofibers as a Function of Molecular Weight and Processing Parameters. *J. Appl. Polym. Sci.* **2008**, *108* (1), 308−319.
(34) Haider, A.; Haider, S.; Kang, I. K. A Comprehensive Review Summarizing the Effect of Electrospinning Parameters and Potential Applications of Nanofibers in Biomedical and Biotechnology. *Arab. J. Chem.* **2018**, *11* (8), 1165−1188.
(35) de Oliveira Santos, R. P.; Castro, D. O.; Ruvolo-Filho, A. C.; Frollini, E. Processing and Thermal Properties of Composites Based on Recycled PET, Sisal Fibers, and Renewable Plasticizers. *J. Appl. Polym. Sci.* **2014**, *131* (12), 40386.
(36) Luo, X.; Li, Y. Synthesis and Characterization of Polyols and Polyurethane Foams from PET Waste and Crude Glycerol. *J. Polym. Environ.* **2014**, *22*, 318−328.
(37) Boschmeier, E.; Archodoulaki, V. M.; Schwaighofer, A.; Lendl, B.; Bartl, A. A Novel Quantification Tool for Elastane in Textiles Using Thermal Treatment. *Polym. Test.* **2023**, *118*, No. 107920.
(38) Sáenz-Pérez, M.; Laza, J. M.; García-Barrasa, J.; Vilas, J. L.; León, L. M. Influence of the Soft Segment Nature on the Thermomechanical Behavior of Shape Memory Polyurethanes. *Polym. Eng. Sci.* **2018**, *58* (2), 238−244.
(39) Cervantes-Uc, J. M.; Espinosa, J. I. M.; Cauich-Rodríguez, J. V.; Avila-Ortega, A.; Vázquez-Torres, H.; Marcos-Fernández, A.; San Román, J. TGA/FTIR Studies of Segmented Aliphatic Polyurethanes and Their Nanocomposites Prepared with Commercial Montmorillonites. *Polym. Degrad. Stab.* **2009**, *94* (10), 1666−1677.
(40) Martone, A.; Giordano, M.; Antonucci, V.; Zarrelli, M. Enhancing Damping Features of Advanced Polymer Composites by Micromechanical Hybridization. *Composites, Part A* **2011**, *42* (11), 1663−1672.
(41) Blaga, A.; Feldman, D. Morphology of Polyurethane Modified by Plasticizing, Blending, or Reinforcing. *J. Appl. Polym. Sci.* **1983**, *28* (3), 1033−1044.
(42) Niesten, M. C. E. J.; Krijgsman, J.; Harkema, S.; Gaymans, R. J. Melt Spinnable Spandex Fibers from Segmented Copolyetheresteraramids. *J. Appl. Polym. Sci.* **2001**, *82* (9), 2194−2203.
(43) Xu, W.; Zhang, R.; Liu, W.; Zhu, J.; Dong, X.; Guo, H.; Hu, G. H. A Multiscale Investigation on the Mechanism of Shape Recovery for IPDI to PPDI Hard Segment Substitution in Polyurethane. *Macromolecules* **2016**, *49* (16), 5931−5944.
(44) Zhu, Y.; Hu, J.; Yeung, L. Y.; Lu, J.; Meng, Q.; Chen, S.; Yeung, K. Effect of Steaming on Shape Memory Polyurethane Fibers with Various Hard Segment Contents. *Smart Mater. Struct.* **2007**, *16* (4), 969.
(45) Strain, I. N.; Wu, Q.; Pourrahimi, A. M.; Hedenqvist, M. S.; Olsson, R. T.; Andersson, R. L. Electrospinning of Recycled PET to Generate Tough Mesomorphic Fibre Membranes for Smoke Filtration. *J. Mater. Chem. A* **2015**, *3* (4), 1632−1640.
(46) Sasaki, T.; Morino, D.; Tabata, N. Origin of Enhanced Cold Crystallization Rate for Freeze-dried Poly (L-lactide) from Solutions. *Polym. Eng. Sci.* **2011**, *51* (9), 1858−1865.
(47) Pawlak, A. The Entanglements of Macromolecules and Their Influence on the Properties of Polymers. *Macromol. Chem. Phys.* **2019**, *220* (10), No. 1900043.
(48) Rao, M. V. S.; Dweltz, N. E. Influence of Molecular Weight on the Ordered State in Poly (Ethylene Terephthalate). *J. Appl. Polym. Sci.* **1986**, *31* (5), 1239−1249.
(49) Samios, C. K.; Gravalos, K. G.; Kalfoglou, N. K. In Situ Compatibilization of Polyurethane with Poly (Ethylene Terephthalate). *Eur. Polym. J.* **2000**, *36* (5), 937−947.

(50) Marchant, R. E.; Zhao, Q.; Anderson, J. M.; Hiltner, A. Degradation of a Poly (Ether Urethane Urea) Elastomer: Infra-red and XPS Studies. *Polymer* **1987**, *28* (12), 2032−2039.
(51) Vesel, A.; Mozetic, M.; Zalar, A. XPS Study of Oxygen Plasma Activated PET. *Vacuum* **2007**, *82* (2), 248−251.
(52) Mu, X.; Zhan, J.; Feng, X.; Yuan, B.; Qiu, S.; Song, L.; Hu, Y. Novel Melamine/o-Phthalaldehyde Covalent Organic Frameworks Nanosheets: Enhancement Flame Retardant and Mechanical Performances of Thermoplastic Polyurethanes. *ACS Appl. Mater. Interfaces* **2017**, *9* (27), 23017−23026.
(53) Wagner, C. D.; Naumkin, A. V.; Kraut-Vass, A.; Allison, J. W.; Powell, C. J.; Rumble, J. R., Jr. *NIST Standard Reference Database 23. Reference Fluid Thermodynamic and Transport Properties* National Institute of Standards and Technology; 2003.
(54) Morgan, S. E.; Willis, M. L.; Dianat, G.; Peterson, G. W.; Mahle, J. J.; Parsons, G. N. Toxin-Blocking Textiles: Rapid, Benign, Roll-to-roll Production of Robust MOF-Fabric Composites for Organophosphate Separation and Hydrolysis. *ChemSusChem* **2023**, *16* (2), No. e202201744.
(55) Li, G.; Zhao, Y.; Lv, M.; Shi, Y.; Cao, D. Super Hydrophilic Poly (Ethylene Terephthalate)(PET)/Poly (Vinyl Alcohol)(PVA) Composite Fibrous Mats with Improved Mechanical Properties Prepared via Electrospinning Process. *Colloids Surf., A* **2013**, *436*, 417−424.
(56) Amrollahi, M.; Sadeghi, G. M. M. Assessment of Adhesion and Surface Properties of Polyurethane Coatings Based on Non-Polar and Hydrophobic Soft Segment. *Prog. Org. Coat.* **2016**, *93*, 23−33.
(57) Jasmee, S.; Omar, G.; Masripan, N. A. B.; Kamarolzaman, A. A.; Ashikin, A. S.; Ani, F. C. Hydrophobicity Performance of Polyethylene Terephthalate (PET) and Thermoplastic Polyurethane (TPU) with Thermal Effect. *Mater. Res. Express* **2018**, *5* (9), No. 096304.
(58) Uyar, T.; Besenbacher, F. Electrospinning of Uniform Polystyrene Fibers: The Effect of Solvent Conductivity. *Polymer* **2008**, *49* (24), 5336−5343.
(59) Lin, J.; Shang, Y.; Ding, B.; Yang, J.; Yu, J.; Al-Deyab, S. S. Nanoporous Polystyrene Fibers for Oil Spill Cleanup. *Mar. Pollut. Bull.* **2012**, *64* (2), 347−352.
(60) Wu, J.; Wang, N.; Wang, L.; Dong, H.; Zhao, Y.; Jiang, L. Electrospun Porous Structure Fibrous Film with High Oil Adsorption Capacity. *ACS Appl. Mater. Interfaces* **2012**, *4* (6), 3207−3212.
(61) Sarbatly, R.; Krishnaiah, D.; Kamin, Z. A Review of Polymer Nanofibres by Electrospinning and Their Application in Oil−Water Separation for Cleaning up Marine Oil Spills. *Mar. Pollut. Bull.* **2016**, *106* (1−2), 8−16.
(62) Elmaghraby, N. A.; Omer, A. M.; Kenawy, E. R.; Gaber, M.; Ragab, S.; Nemr, A. El. Composite Nanofiber Formation Using a Mixture of Cellulose Acetate and Activated Carbon for Oil Spill Treatment. *Environ. Sci. Pollut. Res.* **2023**, *30* (13), 38683−38699.
(63) Elmaghraby, N. A.; Omer, A. M.; Kenawy, E. R.; Gaber, M.; El Nemr, A. Fabrication of Cellulose Acetate/Cellulose Nitrate/Carbon Black Nanofiber Composite for Oil Spill Treatment. *Biomass Convers. Biorefin.* **2022**, 1−19, DOI: 10.1007/s13399-022-03506-w.
(64) Topuz, F.; Abdulhamid, M. A.; Nunes, S. P.; Szekely, G. Hierarchically Porous Electrospun Nanofibrous Mats Produced from Intrinsically Microporous Fluorinated Polyimide for the Removal of Oils and Non-Polar Solvents. *Environ. Sci.: Nano* **2020**, *7* (5), 1365−1372.
(65) Dong, T.; Ye, H.; Wang, W.; Zhang, Y.; Han, G.; Peng, F.; Lou, C. W.; Chi, S.; Liu, Y.; Liu, C.; Lin, J. H. A Sustainable Layered Nanofiber/Sheet Aerogels Enabling Repeated Life Cycles for Effective Oil/Water Separation. *J. Hazard. Mater.* **2023**, *454*, No. 131474.
(66) Wu, D.; Fang, L.; Qin, Y.; Wu, W.; Mao, C.; Zhu, H. Oil Sorbents with High Sorption Capacity, Oil/Water Selectivity and Reusability for Oil Spill Cleanup. *Mar. Pollut. Bull.* **2014**, *84* (1−2), 263−267.
(67) Yin, K.; Wang, Y.; Zhao, H.; Wang, D.; Guo, M.; Mu, M.; Liu, Y.; Nie, X.; Li, B.; Li, J.; Xing, M. A Comparative Review of Microplastics and Nanoplastics: Toxicity Hazards on Digestive, Reproductive and Nervous System. *Sci. Total Environ.* **2021**, *774*, No. 145758.

https://doi.org/10.1021/acsapm.4c00916
ACS Appl. Polym. Mater. 2024, 6, 8798−8810